Microscopic Structure and Microscopic Environment of a Polyfluorinated Surfactant/Clay Hybrid Compound: Photochemical Studies of Rose Bengal

ARTICLE *in* LANGMUIR · APRIL 2002

Impact Factor: 4.46 · DOI: 10.1021/la011697k

6 AUTHORS, INCLUDING:

Tatsuto Yui
Tokyo Metropolitan University
65 PUBLICATIONS **1,361** CITATIONS
SEE PROFILE

Donald A. Tryk
University of Yamanashi
249 PUBLICATIONS **15,474** CITATIONS
SEE PROFILE

Microscopic Structure and Microscopic Environment of a Polyfluorinated Surfactant/Clay Hybrid Compound: Photochemical Studies of Rose Bengal

Tatsuto Yui,[†] Sundara Rajan Uppili,[‡] Tetsuya Shimada,[†] Donald A. Tryk,[†] Hirohisa Yoshida,[†] and Haruo Inoue*[,†,§]

Department of Applied Chemistry, Graduate Course of Engineering, Tokyo Metropolitan University, 1-1 Minami-ohsawa, Hachiohji-City, Tokyo 192-0397, Japan, Department of Chemistry, Tulane University, New Orleans, Louisiana 70118, and CREST (Japan Science and Technology)

Received November 20, 2001. In Final Form: February 25, 2002

The microenvironments of a series of polyfluorinated surfactants [$C_nF_{2n+1}CONH(CH_2)_2N^+(CH_3)_2C_{16}H_{33}$ Br^-; designated as C*n*F−S, where $n = 1-3$]/clay (saponite) hybrid compounds dispersed in water-saturated benzene were investigated based on the photochemical behavior of Rose Bengal (RB) as a probe molecule. A small-angle X-ray scattering study showed that the interlayer distance (clearance space) of the C3F−S/clay hybrid compounds was expanded up to 3.8 nm by the dispersion in water-saturated benzene from the original distance of 3.0 nm for the dried hybrid compound, indicating expansion of the hybrid compound upon swelling with the solvent benzene. The RB molecules are proposed to form ion-association complexes with the C*n*F−S surfactant, most likely existing in the vicinity of the ammonium group of the surfactant intercalated in the cation-exchangeable clay saponite. The absorption and fluorescence maxima of RB intercalated in the hybrid compounds were significantly red-shifted from those in aqueous solution. The hybrid compounds provide an environment with polarity between that of ethyl acetate and 1-butanol. The microscopic polarity of the hybrid compounds depends on the fluorocarbon chain length (*n*) of the surfactant, and the polarities increase with increasing fluorocarbon chain length. On the basis of the observed photochemical behavior of RB, including the relative decomposition rates, excited triplet lifetimes, and relative excited triplet quantum yields, the microscopic concentration of water in the hybrid layer was estimated to decrease in the order C3F−S > C2F−S > C1F−S. These differences are discussed in relation to differences in the microscopic orientational structure of the polyfluorinated surfactant within the clay layer.

Introduction

Clays are alumino-silicate minerals that possess lamellar structures. Depending on the composition, the surfaces can be either positively or negatively charged; the latter are examined in the present work. Various types of electrically charged molecules can be incorporated into the interlayer space in the intercalation process due to substantial stabilization by charge neutralization.[1−4] These microscopically closed cavity systems hold much interest from the viewpoint of chemical reaction microenvironments,[5−7] with specific applications involving catalysts,[8] molecular recognition,[9] stereospecific control of intercalants,[10] and others.[11−13] The intercalation of alkylammonium derivatives has been particularly well examined, and these derivatives have been utilized in a wide variety of applications.[14−18] Intercalated surfactant-type molecules form molecular assemblies in the interlayer space, due to attractive interactions between the long alkyl chains of the molecules.[5−7,14−18]

Fluorocarbons and their derivatives have attracted much interest due to their strong hydrophobicity, lipophobicity, high resistance to oxidation, and high stability in the presence of strong acid and bases. Perfluoro-organic compounds generally exhibit very weak intermolecular interactions with other molecules.[19−21] It has been expected

[†] Tokyo Metropolitan University.
[‡] Tulane University.
[§] CREST (Japan Science and Technology).

(1) Grim, R. E. *Clay Mineralogy*; McGraw-Hill: New York, 1953.
(2) Theng, B. K. *The Chemistry of Clay-Organic Reactions*; Adam Hilger: London, 1974.
(3) Van Olphen, H. *An Introduction to Clay Colloid Chemistry*, 2nd ed.; Wiley-Interscience: New York, 1977.
(4) Shiramizu, H. *Clay Mineralogy*; Asakura-shoten: Tokyo, 1988.
(5) Takagi, K.; Shichi, T. In *Solid State and Surface Photochemistry*; Ramamurthy, V., Schanze, K. S., Eds.; Marcel Dekker: New York, 2000; Vol. 5, p 31.
(6) Shichi, T.; Takagi, K. *J. Photochem. Photobiol., C* **2000**, *1*, 113.
(7) Ogawa, M.; Kuroda, K. *Chem. Rev.* **1995**, *95*, 399.
(8) (a) Shimazu, S.; Hirano, T.; Uematsu, S. *Appl. Catal.* **1987**, *34*, 255. (b) Shimazu, S.; Ro, K.; Sento, T.; Ichikuni, N.; Uematsu, T. *J. Mol. Catal. A: Chem.* **1996**, *107*, 297.
(9) Yamagishi, A. *J. Coord. Chem.* **1987**, *16*, 131.
(10) (a) Usami, H.; Takagi, K.; Sawaki, Y. *J. Chem. Soc., Perkin Trans. 2* **1990**, 1723. (b) Takagi, K.; Shichi, T.; Usami, H.; Sawaki, U. *J. Am. Chem. Soc.* **1993**, *115*, 4339. (c) Sasai, R.; Shin'ya, N.; Shichi, T.; Takagi, K.; Gekko, K. *Langmuir* **1999**, *15*, 413. (d) Sonobe, K.; Kikuta, K.; Takagi, K. *Chem. Mater.* **1999**, *11*, 1089.
(11) Maguran, E. D.; Kieke, M. D.; Reichert, W. W.; Chiavoni, A. *NGLI Spokesman* **1987**, *50*, 453.
(12) Mardis, W. S. *J. Am. Oil Chem. Soc.* **1984**, *61*, 382.
(13) Barrer, R. M. *Philos. Trans. R. Soc. London, Ser. A* **1984**, *344*, 333.
(14) (a) Lagaly, G. *Angew. Chem., Int. Ed. Engl.* **1976**, *15*, 575. (b) Lagaly, G. *Clay Miner.* **1981**, *16*, 1. (c) Lagaly, G. *Clays Clay Miner.* **1982**, *30*, 215.
(15) (a) Weiss, A. *Chem. Ber.* **1958**, *91*, 487. (b) Weiss, A. *Angew. Chem.* **1963**, *75*, 113. (c) Weiss, A. *Angew. Chem., Int. Ed. Engl.* **1963**, *2*, 134.
(16) (a) Vaia, R. A.; Ishii, H.; Giannelis, E. P. *Chem. Mater.* **1993**, *5*, 1694. (b) Vaia, R. A.; Teukolsky, R. K.; Giannelis, E. P. *Chem. Mater.* **1994**, *6*, 1017.
(17) (a) Ogawa, M.; Aono, T.; Kuroda, K.; Kato, C. *Langmuir* **1993**, *9*, 1529. (b) Ogawa, M.; Wada, T.; Kuroda, K. *Langmuir* **1995**, *11*, 4598.
(18) (a) Slade, P. G.; Raupach, M.; Emerson, W. W. *Clays Clay Miner.* **1978**, *26*, 125. (b) Okahata, Y.; Shimazu, A. *Langmuir* **1989**, *5*, 954. (c) Yan, Y.; Bein, T. *Chem. Mater.* **1993**, *5*, 905. (d) Xu, S.; Boyd, S. A. *Langmuir* **1995**, *11*, 2508.
(19) Banks, R. E. *Organofluorine Chemicals and their Industrial Applications*; Ellis Horwood Ltd.: Chichester, U. K., 1979.

10.1021/la011697k CCC: $22.00
Published on Web 04/23/2002

that when they are used as solvents, solute−solute intermolecular interactions would be enhanced.[22,23] Examination of chemical reactions in such perfluorinated environments would be most interesting. In most cases, however, the extremely low solubility of organic compounds in perfluoro-organic compounds means that there is little chance to examine perfluorinated compounds as solvents. One of the most promising approaches to solve this problem would be the formation of polyfluorinated environments in molecular assemblies, such as micelles, reverse micelles, and vesicles, with subsequent examination of chemical reactions in these environments. Polyfluorinated surfactants have indeed been found to form micelles[24] and vesicles[25] with unique fluorinated microenvironments at their interfaces, owing to a delicate balance between hydrophobic and lipophobic interactions of the perfluoroalkyl chain.

With these viewpoints in mind, we have been investigating the intercalation of polyfluorinated surfactants into clay minerals and the resulting surfactant/clay hybrid compounds.[26] Polyfluorinated surfactants are easily intercalated into the clay interlayer spaces and form rigidly packed bilayer structures therein. The C3F−S polyfluorinated surfactants exhibit intercalation up to 440% versus the cation exchange capacity (CEC) as a saturated adsorption limit. The distance between the layers (clearance space) maintains a constant value, and the polyfluorinated surfactants form bilayer structures at intercalation levels from 100 to 440% CEC. These results indicate that the polyfluorinated surfactant/clay hybrid compounds have interlayer spaces (microcavities) of molecular dimensions; the vertical dimension is fixed at ca. 3.0 nm as the clearance space, and the horizontal dimensions can be controlled by variation of the intercalation levels of the surfactant. The schematic structures of the polyfluorinated surfactant (C3F−S)/clay hybrid compounds are shown in Figure 1.

Cavities of such dimensions are very interesting, because they provide polyfluorinated chambers at a molecular scale for chemical reactions. The polyfluorinated surfactant/clay hybrid compounds are well dispersed in benzene, which enables chemical reactions to be conducted in the microcavity in solution phase. This prompted us to study the characteristics of the cavity microenvironments for chemical reactions. In this paper, we report on the cointercalation (with surfactant) of Rose Bengal (RB) and its photochemical behavior in the polyfluorinated microcavity. RB and its derivatives have been well examined for excited-state properties, including singlet oxygen formation,[27−36] aggregation properties,[37−41] photobleaching,[42−44]

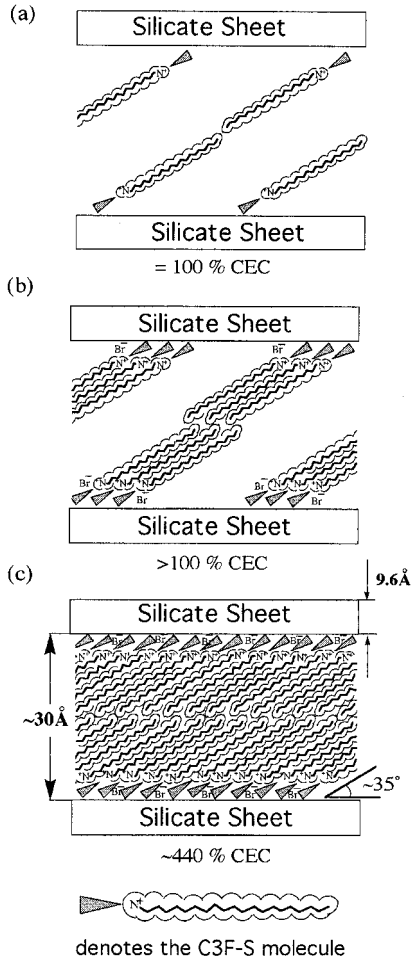

Figure 1. Schematic structure of C3F−S/clay hybrid compounds for various amounts of adsorbed C3F−S molecules: (a) amount approximately equal to CEC; (b) amounts in excess of CEC; and (c) 440% CEC. Under the conditions depicted in (a) or (b), the polyfluorinated surfactant/clay hybrid compounds have molecular size microcavities in the interlayer. The intercalation level of surfactant controls the size of the microcavity.

use as a photochemical probe,[24,25,44−48] and others.[49,50] On the basis of this photochemical behavior, the microscopic

(20) Negishi, A. *Chemistry of Fluorine*; Maruzen: Tokyo, 1988.
(21) Kitazumi, T.; Ishihara, T.; Taguchi, T. *Chemistry of Fluorine*; Kodansha Scientific: Tokyo, 1993.
(22) Briks, J. B.; Christophorou, L. G. *Photophysics of Aromatic Molecules*; Birks, J. B., Ed.; John Wiley & Sons Ltd.; New York, 1969; Chapter 4.
(23) Lawson, C. W.; Hirayama, F.; Lipsky, S. *J. Chem. Phys.* **1969**, *51*, 1590.
(24) Kameo, Y.; Takahashi, S.; Kowald, M. K.; Ohmachi, T.; Takagi, S.; Inoue, H. *J. Phys. Chem. B* **1999**, *103*, 9562.
(25) Kusaka, H.; Uno, M.; Kowald, M. K.; Ohmachi, T.; Kidokoro, S.; Yui, T.; Takagi, S.; Inoue, H. *Phys. Chem. Chem. Phys.* **1999**, *1*, 3135.
(26) Yui, T.; Yoshida, H.; Tachibana, H.; Tryk, D. A.; Inoue, H. *Langmuir* **2002**, *18*, 891.
(27) Nemoto, M.; Kokubun, H.; Koizumi, M. *Bull. Chem. Soc. Jpn.* **1969**, *42*, 2464.
(28) Fleming, G. R.; Knight, A. W.; Morris, J. M.; Morrison, R. J. S.; Robinson, G. W. *J. Am. Chem. Soc.* **1977**, *99*, 4306.
(29) Craner, L. E.; Spears, K. G. *J. Am. Chem. Soc.* **1978**, *100*, 221.
(30) (a) Gollnick, K.; Fouda, M. F. R. *Tetrahedron Lett.* **1981**, *22*, 4053. (b) Gollnic, K.; Schenck, G. O. *Pure Appl. Chem.* **1964**, *9*, 507.
(31) Rodgers, M. A. J. *Chem. Phys. Lett.* **1981**, *78*, 509.
(32) Gabdin, E.; Lion, Y.; Van de Vorst, A. *Photochem. Photobiol.* **1983**, *37*, 271.
(33) Lamberts, J. J. M.; Schumacher, D. R.; Neckers, D. C. *J. Am. Chem. Soc.* **1984**, *106*, 5879.
(34) Gottschalk, P.; Paczkowski, J.; Neckers, D. C. *J. Photochem.* **1986**, *35*, 277.
(35) Neckers, D. C. *J. Photochem. Photobiol., A* **1989**, *47*, 1.
(36) Lamberts, J. J. M.; Neckers, D. C. *Tetrahedron* **1985**, *41*, 2183.
(37) Rohatgi, K. K.; Mukhopadhyay, A. K. *J. Indian Chem. Soc.* **1972**, *49*, 1311.
(38) Xu, D.; Neckers, D. C. *J. Photochem. Photobiol., A* **1987**, *40*, 361.
(39) Valdes-Aguilera, O.; Neckers, D. C. *J. Phys. Chem.* **1988**, *92*, 4286.
(40) Valdes-Aguilera, O.; Neckers, D. C. *Acc. Chem. Res.* **1989**, *22*, 171.
(41) Luttrull, D. K.; Valdes-Aguilera, O.; Linden, S. M.; Paczkowski, J.; Neckers, D. C. *Photochem. Photobiol.* **1988**, *47*, 551.
(42) Koizumi, M. *Mol. Photochem.* **1972**, *4*, 57.
(43) Chesneau, E.; Neckers, D. C. *J. Photochem. Photobiol., A* **1988**, *42*, 269.
(44) Bilski, P.; Dabestani, R.; Chignell, C. F. *J. Phys. Chem.* **1991**, *95*, 5784.
(45) Lee, P. C. C.; Rodgers, A. J. *Photochem. Photobiol.* **1987**, *45*, 79.
(46) Bilski, P.; Motten, A. G.; Bilska, M.; Chignell, C. F. *Photochem. Photobiol.* **1993**, *58*, 11.
(47) Bilski, P.; Chignell, C. F. *J. Photochem. Photobiol., A* **1994**, *77*, 49.
(48) Bilski, P.; Dabestani, R.; Chignell, C. F. *J. Photochem. Photobiol., A* **1994**, *77*, 121.

Chart 1

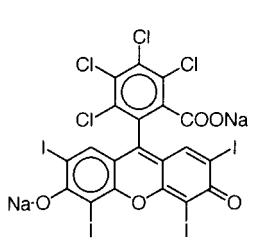

Rose Bengal (RB)

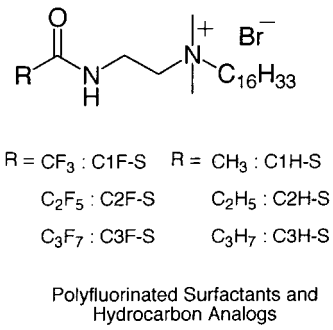

Polyfluorinated Surfactants and Hydrocarbon Analogs

environments of the polyfluorinated surfactant/clay hybrid compounds were characterized.

Experimental Section

Materials. The synthesis of polyfluorinated surfactants (C*n*F−S) and their hydrocarbon analogues (C*n*H−S) has been reported elsewhere.[24] The symbol *n* denotes the number of carbons in the acyl group; F indicates a polyfluorinated surfactant, H a hydrocarbon analogue, and S a surfactant type with a single long alkyl chain. Cetyltrimethylammonium bromide (CTAB; WAKO Pure Chemical Industries, Co.) was recrystallized from acetone three times. Rose Bengal (TCI) was used as received. Cation-exchangeable clay (Sumecton SA) was kindly provided by Kunimine Industries and was used as received. Sumecton SA is a type of sodium saponite synthesized via a hydrothermal reaction. The characteristics of Sumecton SA are as follows:[10a,51] the composition is $[(Si_{7.20}Al_{0.80})(Mg_{5.97}Al_{0.03})O_{20}(OH)_4]^{-0.77}(Na_{0.49}Mg_{0.14})^{+0.77}$; the surface area is 750 $m^2\ g^{-1}$; the cation exchange capacity (CEC) is 0.997 $mequiv\ g^{-1}$; the mean particle size is 0.2−1 μm. The structures of the C*n*F−S and C*n*H−S surfactants and of Rose Bengal (RB) are shown in Chart 1. Deionized water (conductivity < 0.02 $\mu S\ cm^{-1}$) was used as a solvent.

Sample Preparation. The syntheses of the surfactant/clay hybrid compounds were carried out according to the following procedure.[26] As a typical condition, 60 mL of aqueous surfactant solution (5 mM) and 2 mL of aqueous RB solution (2.5×10^{-4} M) were added to 20 mL of aqueous clay dispersion (5 $g\ L^{-1}$). Under these conditions, the loading levels (amounts) of surfactant and RB were 300% and 0.5% with respect to the CEC of the clay, respectively. Control of the surfactant loading levels allowed control of the adsorbed surfactant level. An aqueous mixture of RB/surfactant/clay was stirred at 60−70 °C for 3 h. The precipitate was filtered (ADVANTEC, Toyo Roshi Kaisha, Ltd.; pore size = 0.2 μm), washed well with water on filter paper, and then dried in air at 80 °C to constant weight. The compositions of the surfactant/clay hybrid compounds were determined from the weight gain of the clay and were confirmed by elemental analysis and thermogravimetric analysis (TGA).[26] The amount of adsorbed RB was calculated from the residual amount of RB in the filtrate solution.

Instrumentation and Methods. The solid surfactant/clay hybrid compounds were dispersed in benzene in order to allow measurement of absorption, emission, laser flash photolysis, and photodecomposition, the latter via steady-state photoirradiation. The benzene dispersion of hybrid compounds was carried out by addition of the dried solid hybrid compound to benzene saturated with water and sonication for 3 h at room temperature. The deaerated samples were prepared by seven freeze−pump−thaw deaeration cycles and sealed off under vacuum (ca. 1×10^{-5} Torr).

Absorption and Emission Spectra. Approximately 3 mg of surfactant/clay/RB hybrid compound were dispersed in 10 mL of benzene for absorption and emission measurements, in a 1 × 1-cm path length quartz cell. The excitation wavelength was 520 nm. The absorption spectra were recorded on UV-2100 (Shimadzu) spectrophotometer. The steady-state emission spectra were measured on a F-4010 spectrofluorometer (Hitachi).

Photobleaching during Steady-State Light Irradiation. Approximately 30 mg of hybrid compound was dispersed in 5 mL of benzene saturated with water. The samples were placed in a 4.5-cm path length quartz cell, and their absorbance was measured as a function of irradiation time. A 500-W high-pressure mercury arc lamp, together with a filter system consisting of a 530-nm sharp cutoff filter (Toshiba, VY-53) and a 560-nm interference filter (Toshiba, KL-53), was used as a light source, which allows radiation with 560-nm monochromatic light (full width at half-maximum (fwhm) = 15 nm).

Laser Flash Photolysis. A hybrid compound/benzene dispersion (ca. 30 mg in 5 mL) was prepared. The Xe pulse flash lamp (Tokyo Instruments XF-80; XeCl, 12 ns fwhm) was used as a monitor light source. The light was monitored with a monochromator (RITSU OYO KOGAKU, MC-30) and photomultiplier (Hamamatsu, R-636). The signals were recorded on an oscilloscope (GOULD DSO 4072). The excitation wavelength was 532 nm, the monitored wavelength was 610 nm, and the laser power was less than 1.7 mJ cm^{-2}. The absorption spectra due to RB were found to be unchanged after laser irradiation.

X-ray Analysis. X-ray diffraction (XRD) measurements on the powdered samples were performed on a M21X (MAC Co., Ltd.) diffractometer with monochromatic Cu Kα radiation (λ = 0.15405 nm). A small-angle X-ray scattering (SAXS) instrument was attached to the small-angle X-ray scattering optics (DSC-SRXRD) at beam-line BL-10C at the Photon Factory (PF), High Energy Accelerator Research Organization (KEK), Tsukuba, Japan. The wavelength of the monochromatic X-rays for DSC-SRXRD was 0.1488 nm. The scattered X-rays were detected by a one-dimensional position-sensitive proportional counter (PSPC). The distance between the specimen and the PSPC was 680 nm, which covered 1.25 nm < $S^{-1} = ((2/\lambda) \sin \theta)^{-1}$ < 200 nm, where 2θ is the scattering angle and λ is the X-ray wavelength.

Results and Discussion

Formation of Clay/Surfactant Hybrid Compounds and Cointercalation of RB. The reaction of the aqueous solution of surfactant + RB with the aqueous clay dispersion produces a red precipitate. Intercalation of surfactant was confirmed, principally by weight gain and elemental analysis, as described in the Experimental Section. The amounts of both surfactant and RB intercalated into the clay and the layer distances of the hybrid compounds prepared at various surfactant loading levels are listed in Table 1. The amounts of surfactant incorporated and the corresponding clearance spaces were unaffected by the presence of RB.[26] This indicates that the RB molecule at the very light loading used in the present work (0.5% vs CEC) does not disturb the structure of the hybrid compound.

The anionic RB itself does not intercalate into a cation-exchange-type clay (Sumecton SA) without assistance; destabilization due to Coulombic repulsion between the negative charge of RB and the negative charge on the clay surface prevents the direct intercalation. However, RB is readily intercalated in the presence of an ammonium cation-type surfactant. This can be rationalized by the formation of an ionic association complex[24,44,52] between the cationic surfactant and RB, as evidenced by the following result. RB forms a precipitate in an aqueous surfactant solution below the critical micellar concentration (cmc, ca. 10^{-5} M) of the surfactant but is solubilized in surfactant solutions above the cmc.[24] The anionic RB is thought to associate with the ammonium group of the surfactants and thus to be cointercalated in this manner.

(49) Murasecco-Suardi, P.; Gassmann, E.; Braun, A. M.; Oliveros, E. *Helv. Chim. Acta* **1987**, *70*, 1760.

(50) Linden, S. M.; Neckers, D. C. *Photochem. Photobiol.* **1988**, *47*, 543.

(51) (a) Takagi, S.; Shimada, T.; Yui, T.; Inoue, H. *Chem. Lett.* **2001**, 128. (b) Takagi, S.; Shimada, T.; Eguchi, M.; Yui, T.; Yoshida, H.; Tryk, D. A.; Inoue, H. *Langmuir* **2002**, *18*, 2265.

(52) Yamaguchi, Y.; Yui, T.; Takagi, S.; Shimada, T.; Inoue, H. *Chem. Lett.* **2001**, 644.

Table 1. Structural Data of RB/Surfactant/Clay Hybrid Compounds

	loading level, %CEC	adsorbed amount of surfactant, %CEC	adsorbed amount of RB, loading[a] %	CLS,[b] nm
C3F−S	1000	430	86	3.1
	700	340	>100	3.0
	300	240	>100	3.0
C2F−S	700	230	>100	3.0
	300	210	>100	3.0
CIF−S	700	190	74	3.3
	300	180	>100	3.1
C3H−S	1000	190	34	3.1
	700	180	52	3.2
	300	180	90	3.1
	200	150	>100	3.0
C2H−S	700	170	33	3.2
	300	180	88	3.1
C1H−S	700	190	27	3.3
	300	190	88	3.1
CTAB	1000	230	73	1.2
	300	190	90	1.1

[a] The RB loading level was 0.5% CEC. [b] Clearance space, estimated from subtraction of the layer thickness (0.96 nm) from the *d*(001) values obtained from XRD analysis.

In a comparison of the amounts of incorporated RB for a given surfactant, the amounts of RB decreased with increasing amounts of incorporated surfactant. As already mentioned, the RB molecules are expected to exist in proximity to the ammonium (N^+) group. Differences in the amounts of RB accepted into or rejected from the interlayer should reflect the density and packing structure of the incorporated molecules for a given loading level. Hence, the area surrounding the ammonium groups can become increasingly close-packed with increasing amounts of incorporated surfactant, and thus, it is thought that at high surfactant intercalation levels, the RB molecules can be excluded from the interlayer space principally by steric repulsion, as well as anion−anion repulsion between RB and the negatively charged clay surfaces.

Swelling Behavior of the Polyfluorinated Surfactant/Clay Hybrid Compounds. When the polyfluorinated surfactant/clay hybrid compounds are dispersed in benzene saturated with water, the resultant solution is sufficiently transparent for several hours, even though precipitation is observed on standing overnight. The transparency is thought to be caused by both the matching of the refractive index of benzene (n_D = 1.49792 at 25 °C)[53] with that of clay and a presumed swelling of the hybrid compounds with the solvent benzene. The clay (saponite) itself is well-known to swell with water.[54−56] In contrast, the hybrid compounds are not dispersed in water and remain as a precipitate. The long alkyl chains and the short perfluoroalkyl chains of the polyfluorinated surfactants intercalated in the interlayer space of clay are considered to prevent the swelling with water. The good dispersion of the hybrid compounds in benzene, however, strongly suggests that adequate swelling occurs with this solvent. To check this point, XRD measurements were carried out on a sample soaked thoroughly in toluene and on the effect of drying the sample. Toluene was used in place of benzene, since the latter was found to be too volatile to be used during the XRD scanning time to obtain

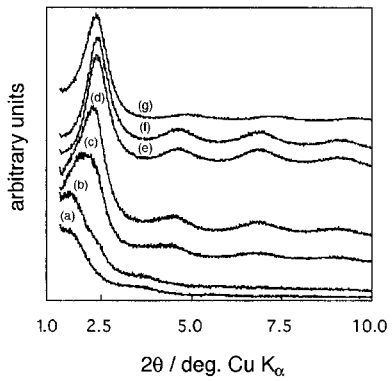

Figure 2. X-ray diffraction profiles of C3F−S/clay hybrid compounds swollen in toluene. The time dependences are caused by evaporation of toluene. Measurements were carried out as a function of time starting from the casting procedure: (a) within 1 min, (b) 6 min, (c) 10 min, (d) 13 min, (e) 30 min, and (f) 50 min; and (g) original hybrid compound (before exposure to toluene).

stable results. Very interestingly, the clearance space of the hybrid compounds expanded to 4.4 nm as a result of swelling in toluene. Furthermore, the layer distance shrank to the original one upon drying; when the wet sample was exposed to air, toluene gradually evaporated, as shown in Figure 2. The reversible expanding and shrinking of the layer distance suggest that the hybrid compound is swelling by incorporation of toluene molecules into the interlayer spaces without changing the bilayer structure. The most interesting point should be how the hybrid compounds are dispersed in benzene and whether the layered structure in benzene is modified or not as compared with that in the dried sample. The SAXS measurements on the C3F−S/clay hybrid sample dispersed in benzene clearly indicate that the clearance space of the hybrid compound is expanded to 3.8 nm in benzene from the original value (3.0 nm) of the dried sample (see Table 1). When benzene dispersions of the hybrid compounds containing RB were filtered through a membrane filter made of Teflon (pore size, 0.2 μm), RB was not observed in the filtrate, indicating that RB associated with the polyfluorinated surfactants remains in the interlayer even when the hybrid compounds are dispersed in benzene. Since the ion-association complex of RB with the polyfluorinated surfactant is more soluble in benzene than the surfactant itself, this result indicates that the surfactants themselves also remain in the interlayer space. Judging from all of these results, we propose that the hybrid compounds incorporate benzene into the interlayer space, resulting in expansion of the layer distance to 3.8 nm, as stated above. The bilayer structure is proposed to be maintained by incorporation of benzene molecules between each layer of surfactant, in a sandwich structure, as shown in Figure 3.

Micropolarity. One of the most fundamental characteristics of these microenvironments is the micropolarity experienced by molecules situated in the microcavity. Rose Bengal is well-known to be sensitive to the polarity of the solvent and is expected to serve as a good probe for estimating the micropolarity of the environment surrounding the molecule.[24,25] Before discussing the micropolarity, attention should be focused on whether RB is intercalated into the interlayer space as an unaggregated species or in an aggregated form. The absorption spectrum of RB undergoes a drastic change with aggregate formation: substantial broadening and change of the spectral shape are observed.[37−41,44] The most characteristic indicator for aggregation is the ratio between the absorption

(53) Riddick, J. A.; Bunger, W. B.; Skano, T. K. *Organic Solvents*; Techniques of Chemistry, Vol. II; John Wiley & Sons: New York, 1986.
(54) Weiss, A. *Angew. Chem., Int. Ed. Engl.* **1981**, *20*, 850.
(55) Thomas, J. T.; Theocharis, C. R. In *Inclusion Compounds*; Atwood, J. L., Davies, J. D., MacNicol, D. D., Eds.; Oxford: London, 1991; Vol. 5, p 104.
(56) Sposito, G.; Prost, R. *Chem. Rev.* **1982**, *82*, 553.

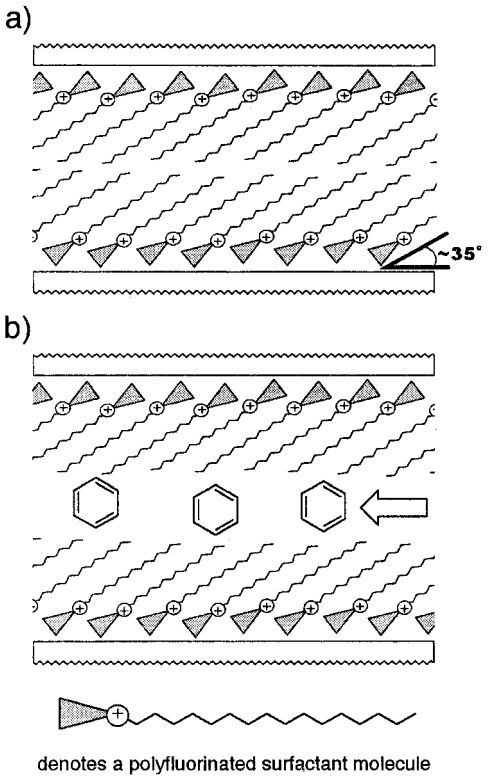

Figure 3. Schematic drawing of polyfluorinated surfactant/clay hybrid compound: (a) solid state and (b) swollen in benzene; the clay layer expands due to incorporation of benzene molecules.

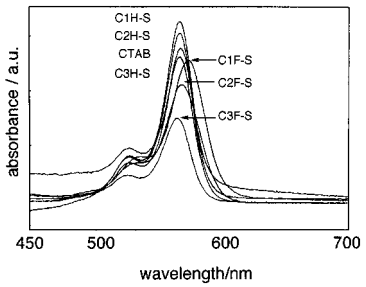

Figure 4. Absorption spectra of RB cointercalated in various surfactant/clay hybrid compounds dispersed in benzene.

intensities of the λ_{max} (P_1) and of the shoulder (P_2) around 500 nm. In aqueous solution, the unaggregated RB at lower concentrations (below 10^{-5} M) has a peak ratio of $P_2/P_1 = 0.32$, while the ratio drastically increases upon aggregation.[37] Since the dimer formation constant K was reported to be 250 M^{-1},[37] RB ([RB] $= 2 \times 10^{-5}$ M) should exist as an unaggregated species under the present experimental conditions in aqueous solution. Absorption spectra for benzene dispersions of RB intercalated in various surfactant/clay hybrid compounds are shown in Figure 4. Their absorption maxima and P_2/P_1 ratios are listed in Table 2. The absorption maxima ($\lambda_{A,max}$) were significantly red-shifted from that in RB aqueous solution (549 nm, see Table 2). However, the spectral shape, P_2/P_1 ratio, and fwhm (28 nm) were almost the same as those in aqueous solution. The fluorescence spectra exhibited the mirror images of the absorption spectra, and no new emission bands (e.g., excimer) were observed.[38] All of these results clearly indicate that the RB molecules exist as essentially unaggregated molecules in the interlayer spaces of these hybrid compounds.

Table 2. Absorption ($\lambda_{A.max}$) and Fluorescence ($\lambda_{F.max}$) Maxima and Peak Ratio (P_2/P_1) of RB and Estimated Dielectric Constant[a] (ϵ) in Surfactant/Clay Hybrid Compounds

	$\lambda_{A.max}$/ nm	$\lambda_{F.max}$[b]/ nm	P_2/P_1	ϵ from $\lambda_{A.max}$	ϵ from $\lambda_{F.max}$
RB(aq)[c]	549	570	0.32		
C1F−S[d]	571	591	0.32	9	6
C2F−S[d]	568	588	0.34	12	8
C3F−S[d]	563	581	0.35	18	18
CIH−S[d]	565	581	0.31	16	18
C2H−S[d]	565	581	0.28	16	18
C3H−S[d]	565	581	0.29	16	18
CTAB[d]	565	582	0.32	15	16

[a] Estimated from calibration relationships of λ_{max} and solvent polarity. [b] Excitation wavelength, 520 nm. [c] RB (2×10^{-6} M) in aqueous solution. [d] Surfactant was loaded at 300% CEC.

The absorption and fluorescence maxima of RB are dependent on the solvent polarity.[28,35,50] In a more polar solvent, the absorption ($\lambda_{A,max}$) and fluorescence emission ($\lambda_{F,max}$) maxima shift to the blue. The following solvents were used to calibrate the relationship between the wavelengths and the polarity, as measured by the dielectric constant ϵ:[24,25] pyridine (ϵ: 12.91), 1-butanol (ϵ: 17.51), 2-propanol (ϵ: 19.92), acetone (ϵ: 20.56), ethanol (ϵ: 24.55), methanol (ϵ: 32.66), and water (ϵ: 78.39).[53] The microscopic polarities of each of the surfactant/clay hybrid compounds were estimated from the absorption and emission maxima, by either interpolation or extrapolation from the λ_{max} versus ϵ calibration graphs just described. The absorption and fluorescence maxima and estimated polarities for all of the surfactant/clay hybrids are shown in Table 2. The micropolarities for each of the hybrid compounds, presumably in the vicinity of the ammonium groups, were significantly smaller than that observed in water, with dielectric constants ranging from 6 to 18. On the basis of the standard values already given, these values correspond to an environment with polarity between that of ethyl acetate ($\epsilon = 6.02$)[53] and 1-butanol. In contrast, the micropolarities of the hydrocarbon-type surfactant series (CnH−S and CTAB) were higher than those of the polyfluorinated surfactants but were the same within the series, even though they had different short hydrocarbon headgroups. In the polyfluorinated surfactant series, these micropolarities increased systematically with increasing length (n) of the short perfluoroalkyl chain. We propose that the more polar C3F−S/clay hybrid compound contains appreciable amounts of water molecules in the vicinity of the ammonium groups. Although the dried samples of the hybrid compounds were revealed to contain almost no water within the interlayers,[26] an extensive study of the adsorption and desorption of water vapor in the solid sample by means of quartz crystal microbalance measurements indicated that ca. 4 molecules of water per surfactant C3F−S molecule are reversibly adsorbed into and desorbed from the interlayer. Since the ammonium groups are well-known to hydrate strongly, the water molecules are proposed to be attached to this group. When the hybrid compounds are dispersed in benzene saturated with water, they are also thought to adsorb water molecules at the ammonium group, since water molecules present at the saturation level in benzene can freely access this site through the expanded interlayer space. The λ_{max} of RB associated with the ammonium group and situated in its vicinity, thus, should be affected by the presence of water molecules bound to the ammonium group, as stated above. The differences in micropolarity of C3F−S, C2F−S, and C1F−S might reflect differences in the microscopic structures of the surfactants in the

Table 3. Relative Decomposition Efficiency ($((dp/dt)_{t=0})_{rel}$), Triplet Lifetime (τ_T), Initial Absorbance (ΔOD_0), and Corrected Decomposition Rate ($((dp/dt)_{t=0})_{rel})/\Delta OD_0$) of RB in Various Systems

	$\tau_T/\mu s$	$[O_2]/10^{-4}$ M	$((dp/dt)_{t=0})_{rel}$	ΔOD_0	$((dp/dt)_{t=0})_{rel}/\Delta OD_0$
RB(aq)[a]	2.5	2.9[f]	1	21.1	47.0
RB(aq)[b]	140−160[e]		0.05	*g*	*g*
C3F−S[c]	1.7	4.5	0.46	11.5	39.9
C3F−S[d]	310		*c*	*g*	*g*
C2F−S[c]	1.9	4.0	0.36	8.1	44.6
CIF−S[c]	3.5	2.2	0.57	6.6	86.8
C3H−S[c]	2.4	3.2	0.08	13.6	5.9
C2H−S[c]	2.3	3.3	0.06	12.7	4.7
C1H−S[c]	3.7	2.1	0.06	*h*	*h*
CTAB[c]	1.3	5.9	0.18	*h*	*h*

[a] [RB] = 2×10^{-5} M in aerated aqueous solution. [b] [RB] = 2×10^{-5} M in deaerated aqueous solution. [c] RB in hybrid compounds under aerated conditions. [d] RB in hybrid compounds under deaerated conditions. [e] Reported value in refs 44, 45, and 49. [f] Reported value in ref 57. [g] Not measured. [h] Not measured due to strong scattering at 532 nm.

clay interlayer space. The relationship between the microscopic structure of the surfactant and the microscopic concentration of water molecules surrounding RB will be described later.

Photochemical Behavior of RB Intercalated in the Surfactant/Clay Hybrid Layer. *Microconcentrations of Oxygen*. Another characteristic piece of information reflecting the microenvironment should be the microconcentration of oxygen. The solubility of oxygen in various solvents is largely dependent upon the nature of the solvent: the concentration of dissolved oxygen in aqueous solution is on the order of $^1/_{10}$ of those in organic solvents,[57] suggesting that the concentration of oxygen serves as a good indicator for hydrophobicity or hydrophilicity of the microenvironment surrounding this probe molecule. For estimating the oxygen microconcentration in the various environments examined here, excited triplet lifetime (τ_T) measurements for RB were carried out by laser flash photolysis. The excited RB triplet states (^{3}RB*) formed by light irradiation are quenched by molecular oxygen.[27−36,42−45] The relationship between ^{3}RB* lifetime and oxygen concentration is given by eq 1.

$$\tau_T = \frac{1}{k_d + k_q[O_2]} \quad (1)$$

Here k_d and k_q denote the deactivation rate constants of RB itself and the quenching rate constant by molecular oxygen, respectively. The excited triplet lifetimes (τ_T) of RB in various environments are listed in Table 3. The τ_T value for RB in deaerated aqueous solutions was reported to be 140−160 μs.[44,45,49] The observed τ_T value for aerated aqueous RB (τ_T = 2.5 μs) was ca. 60 times smaller than that in deaerated aqueous RB; the deactivation of ^{3}RB* was obviously enhanced by dissolved molecular oxygen. The quenching rate constant of ^{3}RB* by molecular oxygen k_q was estimated to be 1.4×10^9 M^{-1} s^{-1}, using the deactivation rate constant under deaerated conditions k_d (= $1/\tau_T$ under deaerated conditions) and the concentration of oxygen in water (2.9×10^{-4} M).[57] The observed k_q value in aqueous solution coincides well with the reported value (1.6×10^9 M^{-1} s^{-1}).[45] The quenching efficiency of ^{3}RB* by molecular oxygen (k_q) in aerated aqueous solution was estimated to be ca. 98%, and the remaining 2% can be assigned to k_d. The τ_T values for the surfactant/clay hybrid compounds varied only slightly from surfactant to surfactant, and all of these values were 83 to 238 times smaller than those observed under deaerated conditions for these C3F−S/clay hybrid compounds. Thus, the quenching efficiencies of ^{3}RB* by molecular oxygen in the hybrid compounds are estimated to be in the range from 98.8% to 99.4%. The microscopic concentrations of molecular oxygen in the hybrids were thus estimated to be in the range from 2.1 to 5.9×10^{-4} M, as listed in Table 3, based on the assumption that the k_q values for the hybrid compounds are the same as those in aqueous solution. These results clearly indicate that the microenvironment surrounding RB is relatively hydrophilic in all of the hybrid compounds.

Photodecomposition of RB. RB is decomposed upon visible light irradiation.[43−45] To probe the characteristics of the microenvironment of the cavity in the interlayer space, the photochemical decomposition of RB in the hybrid compounds was investigated. Extensive studies of the photochemical decomposition have been reported. Neckers et al. reported that some ester derivatives of RB in dichloromethane were more readily decomposed under deaerated conditions than aerated conditions upon visible light irradiation.[43] Bilski et al. observed that azide as a singlet oxygen quencher did not affect the photochemical decomposition of RB in aqueous solution, while the decomposition of eosine was retarded by azide.[44] They also reported that the decomposition of RB was drastically suppressed when solubilized in micelles.[44] Upon visible light irradiation in aerated aqueous solution, RB was shown by Lee et al. to decompose effectively, although it was stable under deaerated conditions.[45] Furthermore, the decomposition was greatly accelerated in aerated D_2O, in which singlet oxygen has a much longer lifetime, by a factor of ca. 10, than in H_2O,[58,59] suggesting that the photochemical decomposition of RB in aqueous solution is caused by singlet oxygen.[45] The photochemical decomposition of RB is clearly dependent on the chemical structure itself, concentration, solvent, and atmosphere: at high dye concentrations, a D−D type mechanism (eq 2) can cause the decomposition, while D−O type mechanisms (eqs 3 and 4) also play an important role under aerated conditions.

$$^3D^* + D \xrightarrow{k_{DD}} D^{+\bullet} + D^{-\bullet} \quad (2)$$

$$^3D^* + {}^3O_2 \xrightarrow{k_{SO}} D^{+\bullet} + O_2{}^{-\bullet} \quad (3)$$

$$^3D^* + {}^3O_2 \xrightarrow{k_{\Delta}} D + {}^1O_2 \quad (4)$$

The reactivity of the photochemical decomposition is thus considered to be governed by a delicate balance between the ratios of the various rate constants, k_{DD}, k_{SO}, and k_{Δ}, the concentrations of the dye itself and that of dissolved oxygen. For probing the microenvironment of the interlayer space in hybrid compounds through the observation of the photochemical decomposition of RB, it should be possible to specify which reaction mechanism is dominant in the present clay/surfactant hybrid system. For this purpose, the photochemical reaction of RB in aqueous solution was carried out under both aerated and deareated conditions. As indicated in Table 3, RB (2×10^{-5} M) was

(57) Steven, L. M.; Carmichael, I.; Hug, G. L. In *Handbook of Photochemistry*, 2nd ed.; Marcel Dekker: New York, 1993; p 289.

(58) (a) Turro, N. J. In *Modern Molecular Photochemistry*; University Science Books: Mill Valley, CA, 1991; Chapter 14. (b) Rodgers, M. A. J.; Snowden, P. T. *J. Am. Chem. Soc.* **1982**, *104*, 5541.

(59) (a) Merkel, P. B.; Kearns, D. R. *J. Am. Chem. Soc.* **1972**, *94*, 1029. (b) Merkel, P. B.; Kearns, D. R. *J. Am. Chem. Soc.* **1972**, *94*, 7244.

Scheme 1

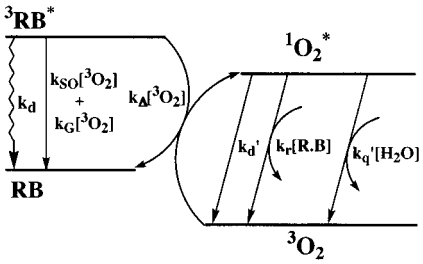

decomposed more efficiently in aerated aqueous solution, by a factor of ca. 20, than in deaerated solution, coinciding well with Lee's observation.[45] The peak intensity ratios (P_2/P_1) of RB clearly indicate that RB exists as an unaggregated species in all of the hybrid environments, as well as in aqueous solution, at the present concentrations, as mentioned above. These results strongly suggest that the singlet oxygen mechanism for the photochemical decomposition is operating as the major reaction pathway, while the D−D mechanism is almost completely suppressed under the present conditions, in which mutual collisions of the separate RB molecules are restricted in the hybrid environment. Assuming the singlet oxygen mechanism, the reaction scheme could be depicted as in Scheme 1. The excited triplet states RB (^{3}RB*) formed by light irradiation are quenched by molecular oxygen, leading to the formation of singlet oxygen ($^1O_2$, rate constant k_Δ), superoxide anion ($O_2^{-\bullet}$, k_{SO}), and ground-state oxygen ($^3O_2$, k_G), respectively. Thus, the quenching rate constant of the triplet excited RB by molecular oxygen (k_q) can be expressed by eq 5.

$$k_q = k_\Delta = k_{SO} = k_G \tag{5}$$

The efficiency of singlet oxygen formation upon the quenching of ^{3}RB* by molecular oxygen can be expressed by eq 6.

$$\alpha = \frac{k_\Delta}{k_\Delta + k_{SO} + k_G} \tag{6}$$

The efficiency (α) has been reported to be around 75%.[30b,32,34,35,45,49] The triplet quenching efficiency by molecular oxygen in the present systems, including aqueous solution and the hybrid environment, is almost quantitative, as shown in Table 3. Singlet oxygen is thus considered to be formed very efficiently and with a similar efficiency in all of the systems examined here. The deactivation of $^1O_2$* includes deactivation of $^1O_2$* itself (k_d'), quenching by water molecules (k_q'), and attack on ground-state RB molecules (k_r). These pathways compete with each other. The RB molecules attacked by $^1O_2$* are oxidatively decomposed and thus bleached. Supposing decomposition mechanisms shown in Scheme 1, the relationship between the photodecomposition quantum yield of RB (Φ_{dec}) and the microconcentration of oxygen can be described by eq 7.

$$\Phi_{dec} = \Phi_{isc}\alpha\left(\frac{k_q[O_2]}{k_d + k_q[O_2]}\right)\beta\left(\frac{k_r[RB]}{k_r[RB] + k_q'[H_2O] + k_d'}\right) \tag{7}$$

Here Φ_{isc}, α, k_d, k_q, β, k_r, k_q', and k_d' denote the intersystem crossing efficiency, the probability of $^1O_2$ formation upon quenching of ^{3}RB* by $^3O_2$, the rate constant for deactivation of 3RB*, the quenching efficiency of ^{3}RB* by molecular oxygen, the decomposition efficiency after RB is attacked by $^1O_2$*, the rate constant for the reaction of $^1O_2$* with RB, the quenching rate constant of $^1O_2$*, and the deactivation rate constant of $^1O_2$*, respectively (Scheme 1). Thus, the RB decomposition efficiency should be inversely dependent on the surrounding water concentration; that is, when the water molecules are concentrated, decomposition of RB should be suppressed due to more efficient quenching of $^1O_2$* by the surrounding water. The microscopic concentration of water molecules in the interlayer space, thus, can be estimated based on the results of the photodecomposition experiment with steady-state light irradiation, as described later.

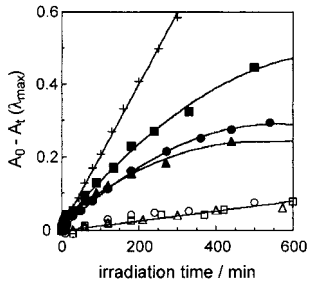

Figure 5. Absorbance change of RB cointercalated in various surfactant/clay hybrid compounds with monochromatic 560-nm light irradiation, under aerated conditions: (●) C3F−S; (▲) C2F−S; (■) C1F−S; (○) C3H−S; (△) C2H−S; (□) C1H−S/clay hybrid compound; (+) aqueous RB.

The absorbance changes of RB induced by the irradiation with monochromatic 560-nm light are shown in Figure 5. The absorbance decreased with irradiation for all systems, indicating decomposition, but the decomposition rates varied over a wide range. In aqueous solution, RB underwent the fastest decomposition, and the absorbance decreased linearly with time. The photochemical behavior of RB intercalated in the surfactant/clay hybrid compounds is summarized in Table 3, including the initial rate of the relative decomposition rate $((dp/dt)_{t=0})_{rel}$ for each surfactant/clay hybrid compound compared to aqueous RB. RB cointercalated in polyfluorinated surfactant/clay hybrids decomposed more slowly in the order C3F−S > C2F−S > C1F−S. The polyfluorinated surfactant (C*n*F−S)/clay hybrids exhibited nonlinearly decreasing absorption, which approached a plateau at ca. 600 min irradiation time. This result may indicate that the diffusion of molecular oxygen is not fully allowed in the hybrid compounds dispersed in benzene compared to aqueous solution. In contrast, the photodecomposition of RB scarcely proceeded in the hydrocarbon-type surfactant (C*n*H−S and CTAB)/clay hybrids; only ca. 5% of the RB was decomposed, even after 600 min light irradiation.

As already stated, the decomposition of RB is thought to be inhibited by water. On the basis of this assumption, it is surprising that the apparent decomposition rate for aqueous RB was greater than that in RB intercalated in any of the surfactant/clay hybrid compounds. Even for the most efficiently decomposing system (C1F−S), the relative rate was only 57% of that in aqueous RB. A likely explanation is that the surfactant/clay hybrid compound provides a special type of environment, distinct from that in aqueous solution.

There are essentially no differences in the singlet oxygen formation efficiencies observed, comparing the hybrid compounds and aerated aqueous solution, as mentioned above. Nevertheless, the decomposition of RB intercalated in the surfactant/clay hybrid compounds was highly inhibited compared to that in aqueous RB. Factors other

than the singlet oxygen formation efficiency should control the reactivity.

Microconcentrations of Water. The RB decomposition quantum yields (Φ_{dec}) are also dependent on the intersystem crossing quantum yield (Φ_{isc}), as indicated in eq 7. The relative Φ_{isc} was directly compared as the initial absorbance at $t = 0$ of ^{3}RB* (ΔOD_0), as shown in Table 3. The largest ΔOD_0 ($= \Phi_{isc}$) in aqueous solution indeed explains the largest overall reactivity. The order of the reactivity in other systems, however, is not completely rationalized by a simple comparison of ΔOD_0 ($= \Phi_{isc}$); C2F−S, C3H−S, and C2H−S showed smaller reactivities than C1F−S despite the larger ΔOD_0 ($= \Phi_{isc}$). The quenching process of $^1O_2$* (k_q'), competing with the oxidative attack on RB (k_r), should be one of the key steps that determine the total reactivity of photodecomposition of RB, as stated above. To discuss this factor in detail, eq 7 was modified to give eq 8. The relative magnitude of Φ_{dec} was estimated from the relative decomposition rate $((dp/dt)_{t=0})_{rel}$.

$$\frac{\Phi_{dec}}{\Phi_{isc}}\left(=\frac{((dp/dt)_{t=0})_{rel}}{\Delta OD_0}\right) = \alpha\beta\left(\frac{k_q[O_2]}{k_d + k_q[O_2]}\right)\left(\frac{k_r[RB]}{k_r[RB] + k_q'[H_2O] + k_d'}\right) = \text{constant}\left(\frac{k_r[RB]}{k_r[RB] + k_q'[H_2O] + k_d'}\right) \quad (8)$$

The relative values of $((dp/dt)_{t=0})_{rel}/\Delta OD_0$ are compared in Table 3 (column 6). As shown in eq 3, the $((dp/dt)_{t=0})_{rel}/\Delta OD_0$ values are functions of $k_q'[H_2O]$. The values should decrease as the magnitude of $k_q'[H_2O]$ increases, due to the number of water molecules surrounding RB increasing. The $((dp/dt)_{t=0})_{rel}/\Delta OD_0$ values decreased systematically in the order C1F−S > C2F−S > C3F−S among the polyfluorinated surfactants. Thus, the $k_q'[H_2O]$ values were estimated to decrease in the order C3F−S > C2F−S > C1F−S. As previously described, the absorption and fluorescence maxima of RB indicate that the micropolarities of the polyfluorinated surfactant/clay hybrid compounds increased with increasing fluorocarbon chain length in the perfluoroalkyl group. The differences in the micropolarity should reflect the microscopic water concentration surrounding RB in the neighborhood of the ammonium group, as observed experimentally. Furthermore, the value of $((dp/dt)_{t=0})_{rel}/\Delta OD_0$ in aqueous solution is larger than those in the hybrid compounds except in the case of C1F−S. These results indicate that the $k_q'[H_2O]$ values in these hybrid environments are larger than that in aqueous solution, even though $[H_2O]$ is clearly very high, being a neat solvent. Therefore, this indicates that an efficient quenching path for $^1O_2$* exists in the hybrid compounds. It is well-known that $^1O_2$* is quenched efficiently by hydroxyl groups.[59,60] We propose that the adsorbed water molecules surrounding RB in the hybrid compounds have a different character compared to that in bulk water; they may have stronger hydrogen bonding formation with $^1O_2$*, since the limited number of adsorbed water molecules may prevent the mutual formation of a full network of hydrogen bonds such as that observed in bulk water. The resultant free hydroxyl groups among the adsorbed water molecules adjacent to RB could quench $^1O_2$* efficiently via strong hydrogen bonding interactions.

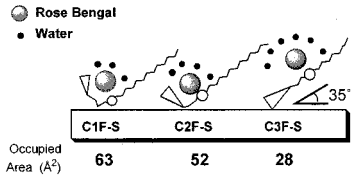

Figure 6. Schematic orientational structure of RB and polyfluorinated surfactants in a clay hybrid layer and corresponding occupied area of each polyfluorinated surfactant.

Microscopic Orientation of Polyfluorinated Surfactant in the Hybrid Layer. Previously, the microscopic orientations of polyfluorinated surfactants in clay hybrid compounds were studied on the basis of the observation of the saturated adsorption limit and the occupied area of each surfactant.[26] The latter were found to be as follows: 63 Å^2 for C1F−S, 52 Å^2 for C2F−S, and 28 Å^2 for C3F−S. The layer distances were all almost the same, even for different perfluoroalkyl chain lengths (see Table 1). From these observations, we conclude that the C1F−S molecule has a large occupied area due to a bent-type structure, leading to a larger "footprint," whereas the C3F−S molecule has a small occupied area due to a linear-type structure and an orientation directed away from the clay surface, as discussed in detail below.[26] The schematic orientational structures of the polyfluorinated surfactant in the clay layer are shown in Figure 6.

The differences in micropolarity and water microconcentration for each of the surfactant/clay hybrid compounds are well understood in relation to the differences in microscopic conformation and orientation of each surfactant. The ammonium group of the C3F−S molecule, which has a linear conformation of the fluorocarbon chain and long alkyl chain, would then be exposed to adsorbed water, increasing the microscopic water concentration and consequently the micropolarity. In contrast, the C1F−S molecule, which has the largest occupied area, should have a bent-type structure. The bending of the fluorocarbon headgroup necessitates proximity of this group to the polar ammonium group, effectively blocking access of water molecules to the RB adjacent to the latter. Thus, the micropolarity and water microconcentration would be expected to decrease. Among the hybrid compounds, C2H−S and C3H−S have very small values of $((dp/dt)_{t=0})_{rel}/\Delta OD_0$, suggesting very efficient quenching of $^1O_2$* in the hydrocarbon-type surfactant/clay hybrid compounds. From a previous study on microscopic orientations, the hydrocarbon-type surfactants were concluded to also have a bent-type structure. Thus, the ammonium groups of the surfactants are attached more closely to the clay surface, where many water molecules are thought to adsorb on the Si−O−Si network. Less hydrophobic short alkyl chains, compared to the short perfluoroalkyl chains, may partly allow the access of water molecules to RB. RB molecules attached to the ammonium group are, thus, concluded to favor larger numbers of water molecules, and $^1O_2$* formed in the neighborhood of RB may undergo very efficient quenching by the water molecules on the clay surface.

LA011697K

(60) Wentworth, P., Jr.; Hones, L. H.; Wentworth, A. D.; Zhu, X.; Larsen, N. A.; Wilson, I. A.; Xu, X.; Goddard, W. A., III; Janda, K. D.; Eschenmoser, A.; Lerner, R. A. *Science* **2001**, *293*, 1806.